Calcite precipitation by *Rhodococcus* sp. isolated from Kotumsar cave, Chhattisgarh, India

Sushmitha Baskar[1,*], Swati Chalia[2] and Ramanathan Baskar[2]

[1]Environmental Studies, School of Interdisciplinary and Transdisciplinary Studies, Indira Gandhi National Open University, New Delhi 110 068, India
[2]Department of Environmental Science and Engineering, Guru Jambheshwar University of Science and Technology, Hisar 125 001, India

The precipitation of carbonate minerals by *Rhodococcus* sp. strain S14 isolated from Kotumsar cave, Chhattisgarh, India is reported. The speleothems at Kotumsar showed high microbial cell enumeration on B4 agar; iron agar (3.4×10^5 CFU/g) and sulphite agar (7.2×10^2 CFU/g). National Centre for Biotechnology Information database was used for the BLASTn sequence search of 16S rRNA sequences. The S14 strain gave similarity scores of ≥99% with the respective organisms on the database. The strain was identified as *Rhodococcus* sp. Culture experiments performed using the isolated strains suggested that the rate of precipitation was dependent on pH, temperature and bacterial growth. *Rhodococcus* sp. S14 strain induced the formation of calcite *in vitro* and the biominerals produced were calcified spherulites with pores (as imaged with SEM). The precipitate, at the end of the experimental period of 35 days, had the appearance of coccoliths. This is the initial report on the possible involvement of *Rhodococcus* sp. in the precipitation of carbonates at Kotumsar cave.

Keywords: Biocalcification, cave geomicrobiology, precipitation, *Rhodococcus* sp.

CAVE environments are characterized by different microorganisms and are sites of microbe–mineral interactions. The composition of the microbial communities in caves is influenced by the geochemistry of the caves, environmental conditions and sedimentary characteristics[1–3]. By performing metabolically versatile functions, microbes influence the biogeochemical cycling of elements and thereby the cave mineral formation[4]. The influence of microorganisms on biomineralization processes is well established[5,6]. Even microbes isolated from diverse environments like soil and water ecosystems (both freshwater as well as saline) are reported to precipitate carbonates. The bacterial influence in the calcareous organisms in marine environment, calcium-rich sediments and cave deposits has been well documented[7–10].

Rhodococcus sp., the Gram-positive, aerobic bacteria belonging to Actinobacteria are found in soil, water and cave environments. They have proven industrially important applications, i.e. they are used for the bioremediation of polychlorinated biphenyls (PCBs), bioactive steroids and acrylamide. The bacteria use a number of organic compounds as energy for their metabolism[11,12].

Due to advances in the molecular methods, it is now established that the microbial diversity in caves or specific habitats cannot be comprehensively studied by traditional culturing methods as only a portion of the existing microbial diversity can be grown *in vitro*[13]. Nevertheless, culture-based approaches help isolate and analyse strains[14]. Then, the isolated strains can be studied by clustering them into operational taxonomic units (OTUs), for comparison with diverse microbial communities isolated globally. Thus, culture-based geomicrobiological studies in combination with the molecular techniques provide an understanding of the 'microbes in action', as microbes that are cultured in the laboratory can be shown as metabolically active in well-defined environmental conditions[15]. *In vitro* culture experiments help enhance our understanding about the capability of the isolated strains to alter the chemistry of their microenvironment (e.g. production of exopolysaccharides (EPS), pH changes, bacterial growth changes) and produce biominerals.

This study focuses on analysing the biomineral capabilities of S14 strain identified as *Rhodococcus* sp. by molecular methods (16S rDNA). The study was performed by: (1) characterizing the culturable heterotrophic microflora from the speleothems; (2) isolating and identifying the mineral-forming bacteria; (3) performing *in vitro* experiments for biomineralization by isolated microbes and (4) analysis of the biomineral using X-ray diffraction (XRD) and scanning electron microscopy (SEM). The combined approach of culture-based experiments along with complementary molecular techniques provides insight into the metabolically active microorganisms.

Study area and geology

Kotumsar cave (18°45′00″–18°56′30″N; 81°51′30″–82°10′00″E) is situated in the Kanger Valley National Park in Bastar district, Chhattisgarh, approximately

*For correspondence. (e-mail: sushmithab@ignou.ac.in)

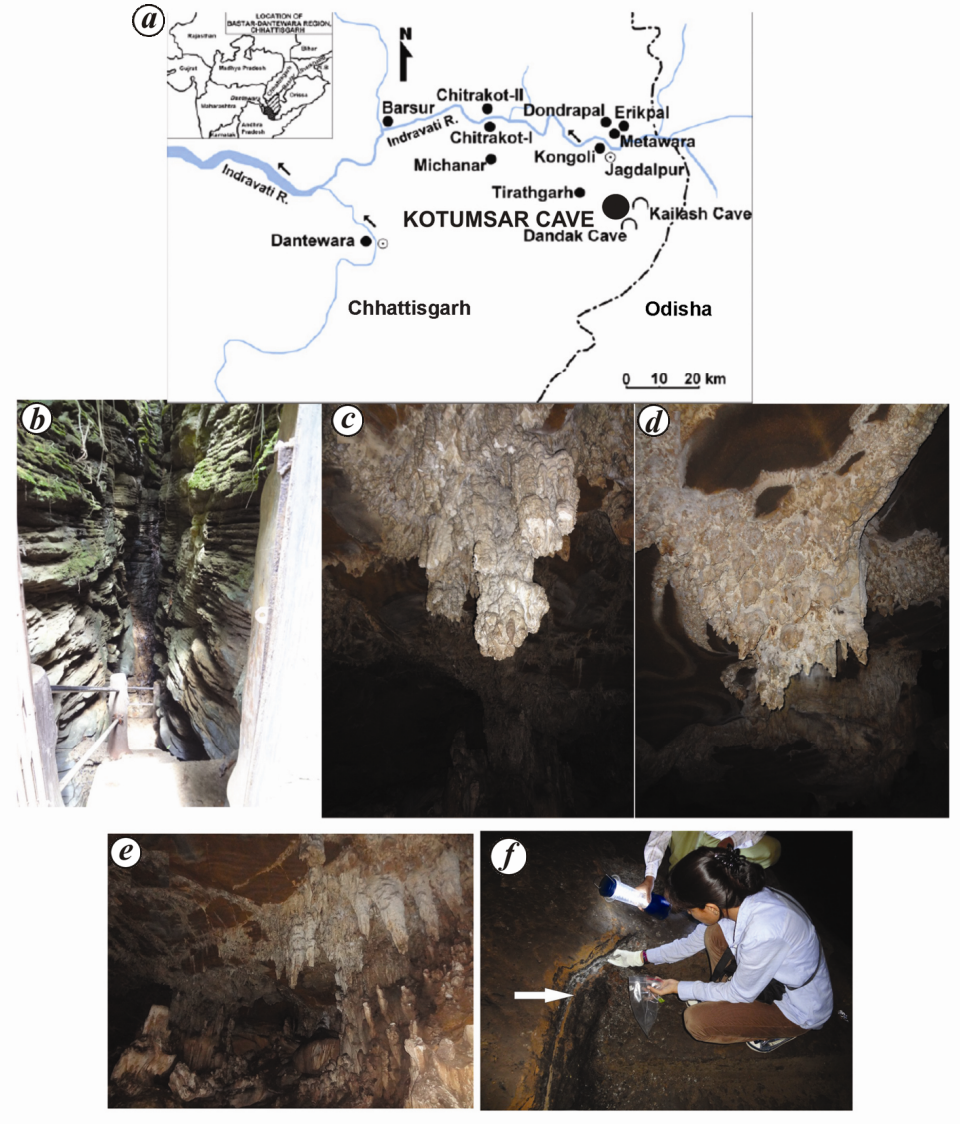

Figure 1. Speleothems from Kotumsar cave, Chhattisgarh, India. ***a***, Map showing position of the study area in India (modified and adapted from Sankhyan *et al.*[16]); ***b***, Entrance to the cave; ***c***, ***d***, stalactites, stalagmites and wall deposits inside the cave; ***e***, Black cave wall deposit KWD3 sampled for the study.

350 km from Raipur, Central India (Figure 1 *a*)[16]. The dissolution of the limestone bedrock resulted in the upper proterozoic Kanger limestone, belonging to the Indravati group[17]. Limestone, purple shale and quartzite are the dominant rock types[17]. Cuddapah group and Vindhyan group rock formations are observed at the Kanger Valley National Park[17]. Kotumsar is reported to be the biologically best known cave in India with a number of highly endemic species at the verge of extinction[18].

Kotumsar is an underground cave, 330 m long, with many chambers and passages that are 20–70 m wide and 55 m deep[19]. The cave entrance is narrow (15 m height) and is 30 m below ground level. The cave exhibits a honey-comb structure, and has several irregular chambers with numerous stalactites (ranging from very small to big 40 ft), stalagmites, wall deposits and draperies (Figure 1 *b*–*f*). Three distinct zones are visible in the cave. The twilight zone runs for 1.5 m followed by a transition and the deep dark aphotic zone. For the present study stalactites, stalagmite, cave wall deposits, drip water and spring water samples (30–280 m from the cave entrance) were collected throughout the length of the cave (Table 1).

Sampling and analytical procedures

Sample collection

Cave deposits and water samples were collected aseptically from minimal contaminated areas in sterile polyurethane bottles and stored at 4°C for further analysis.

Table 1. Details of speleothems sampled from Kotumsar cave, Chhattisgarh

Sample number	Sample type	Characteristics	Temperature (°C)	Humidity (%)	Colour	Zone	Distance from cave entrance (m)	Mineralogy
KWD1	Wall deposit	Hard, dry	25	74	Light brown	Aphotic	70	Calcite
KWD2	Wall deposit	Hard, dry	25	75	Red–brown	Aphotic	90	Calcite
KWD3	Wall deposit	Soft, powdery, moist	27	78	Black	Aphotic	120	Calcite
KSTI	Stalactite	Hard, wet	26	73	Brown	Aphotic	25	Calcite
KST2	Stalactite	Hard, dry	29	78	White	Aphotic	140	Calcite
KST3	Stalactite	Hard, dry	29	80	Brown	Aphotic	280	Calcite
KSM	Stalagmite	Hard, dry	30	80	Blackish-white	Aphotic	280	Calcite

Geochemistry

The major rock geochemistry of the KWD2 and KWD3 deposits (Na_2O, MgO, SiO_2, K_2O, CaO, P_2O_5, Al_2O_3, TiO_2, MnO, Fe_2O_3, LiO) was analysed using an automated sequential X-ray fluorescence spectrometer (WDXRF; BRUKER S8-TIGER X-Ray Spectrometer, Wadia Institute of Himalayan Geology (WIHG), Dehradun). The geochemistry of the water samples (As, B, Ca, Cd, Cr, Cu, Fe, K, Mg, Mn, Na, Ni, P, Pb, S, Zn) was analysed using inductively coupled plasma atomic emission spectroscopy (ICAP-AES; Punjab Agriculture University, Ludhiana). The detection limit of most of the elements analysed is <1 μg/l. Relative standard deviation ranged from 5% to 25%. Merck certiPUR multi-element standards were used to calibrate and standardize the instrument. The total organic carbon content, carbonate, bicarbonate, acidity, alkalinity, hardness, conductivity and pH of spring waters and drip water were determined using standard procedures.

Mineralogy

XRD (X'Pert Pan X-ray diffractometer, Guru Jambheshwar University of Science and Technology, Hisar) and FTIR (RZX; Perkin Elmer, Panjab University, Chandigarh) were used for characterizing the mineral composition.

Electron microscopy

Scanning electron microscopic (SEM) ZEISS EVO 40 EP, resolution, 3.0 nm SE and HV, magnification, 7–1,000,0009; accelerating voltage 0.2–30 kV; WIHG Dehradun) studies were performed on the speleothems and biominerals precipitated *in vitro*. Energy dispersive X-ray spectroscopy (EDX) (EDX microanalyser Bruker LN2 Free X Flash 4010SDD detector; resolution 129 eV at Mn ka9 (5.98 keV; WIHG, Dehradun) was used for quantitative estimation of the chemical composition of the minerals. The detailed protocol followed is according to our earlier studies[10].

Microbiological analysis

Enumeration of microbes on various media

Speleothem samples were crushed in a flamed aseptic mortar and pestle. Serial dilutions in 0.01 M phosphate buffered saline were carried out (pH 7.4; Sigma, St Louis, MO, USA). Aliquots from each dilution series were inoculated into sterile dilute nutrient agar (NA), B4 agar[20], Kliger iron agar, sodium thiosulphate agar, sulphite agar, Mn agar, Bg-11 and iron agar. The detailed protocol followed is according to our earlier studies[10].

In vitro calcite precipitation in B4 liquid media

Fourteen strains (S1–S14) were cultured in B4 liquid medium (calcium acetate 2.5 g l^{-1}, yeast extract 4 g l^{-1}, glucose 10 g l^{-1}, pH 7)[20], for testing *in vitro* calcite precipitation[10]. The changes in pH, bacterial growth and crystal precipitation were observed over a 35 days period. The crystals were analysed using SEM.

Identification of microbial strains

The S14 strain isolated from KWD3 was selected for DNA sequencing identification methods, based on PCR amplification of 16S rRNA genes (16S rDNA) and partial sequencing at geneOmbio Technologies, Pune. This strain was identified using the gene-specific sequencing primers (27F) and ABI BigDye® Terminator v3.1 Cycle Sequencing reaction kit (Applied Biosystems, USA), and the purified PCR amplicons were sequenced. To determine approximate phylogenetic affiliations, partial 16S rRNA gene sequences were analysed with the Basic Local Alignment Search Tool (BLAST) on the NCBI database[21]. The percentage of nucleotide identity and nucleotide-based phylogenetic tree of the strain were established using the MEGA5 program[22] and Bioedit v7.2.1 (ref. 23). The strains S1–S13 were identified in the laboratory using conventional microbiology (Gram stain and biochemical tests).

Table 2. Geochemistry of drip and spring water samples, Kotumsar cave

Sample	KC-D1	KC-D2	KC-D3	KC-S1	KC-S2	KC-S3
Sample type	Drip	Drip	Drip	Spring	Spring	Spring
Collection zone	Twilight	Transition	Aphotic, deep	Twilight	Transition	Aphotic, deep
Distance from cave entrance (m)	30	70	130	80	130	210
pH	6.93	6.93	6.86	6.56	6.51	6.62
Electrical conductivity (mS)	0.32	0.3	0.32	0.27	0.34	0.39
Total dissolved solids (mg/l)	0.16	0.15	0.15	0.12	0.17	0.19
Alkalinity (mg/l)	157.5	200	150	120	137.5	167.5
Bicarbonate (mg/l)	192.2	244	183	146.4	167.8	204.4
Total hardness (mg/l)	172.5	625	550	155	175	222.5
Arsenic	0.001	0.003	0.002	0.003	0.003	0.001
Boron	0.019	0.033	0.125	0.126	0.077	0.109
Calcium	45.35	7.807	15.64	36.01	44.94	57.1
Cadmium	0	0	0	0	0	0
Chromium	0.007	0.007	0.002	0.007	0.001	0.007
Copper	0.017	0.019	0.004	0.014	0.033	0.028
Iron	0.04	0.036	0.025	0.075	0.059	0.041
Potassium	0.448	1.633	1.255	6.273	7.405	4.389
Magnesium	4.428	0.634	0.841	3.424	4.258	3.44
Manganese	0.005	0	0.002	0.001	0	0.001
Sodium	0.852	2.102	2.047	0.679	0.139	1.387
Nickel	0	0.001	0	0.002	0.001	0.001
Phosphorus	0.024	0.057	0.067	0.114	0.06	0.03
Lead	0.013	0.004	0.007	0.021	0.017	0.02
Sulphur	0.868	0.264	0.283	1.522	2.726	1.496
Zinc	0.021	0.027	0.027	0.017	0.004	0.006

Elemental concentration values for metals from arsenic to zinc are in mg/l (Inductively coupled plasma atomic emission spectroscopy, Punjab Agricultural University, Ludhiana).

Table 3. Geochemistry of speleothems from Kotumsar cave

Element	KWD2	KWD3
Na_2O	0.15	0.05%
MgO	0.48	0.50%
Al_2O_3	8.07	6.72%
SiO_2	46.78	79.54%
P_2O_5	8.92	4.39%
K_2O	1.94	1.62%
CaO	6.98	2.76%
TiO_2	0.54	0.44%
MnO	0.006	0.03%
Fe_2O_3	3.05	3.51%
S	5.95	NA
BaO	NA	0.33%
SO_3	NA	0.04%
Cl	NA	0.02%
CuO	NA	0.01%
ZrO_2	NA	98 PPM
ZnO	NA	94 PPM
Cr_2O_3	NA	84 PPM
Rb_2O	NA	75 PPM
NiO	NA	53 PPM
SrO	NA	50 PPM
Y_2O_3	NA	50 PPM
Nb_2O_5	NA	8 PPM
Intensity scale	NA	1,053
SUM	82.87	NA
LOI	16.23	NA
Compton	NA	NA

NA, Not applicable.

Nucleotide sequence accession numbers

Sequences obtained were submitted to the NCBI database (http://www.ncbi.nlm.nih.gov/genebank/), under accession number S14-KU219845.1.

Results

Geochemistry and mineralogy

Elemental concentrations: Analyses of the drip and spring waters showed various trace and major elements (Table 2). Ca concentration in drip and spring waters sampled at different distances and zones along the length of the cave was 7.8–45.35 and 36.01–57.1 mg/l respectively. The total organic carbon content of speleothems ranged from 0.18 to 0.27 wt%. The major oxides present in the cave wall deposit KWD3 showed 2.76% CaO, 3.5% Fe_2O_3, 4.39% P_2O_5, 6.7% Al_2O_3, 98 ppm ZrO_2 and 94 ppm ZnO (Table 3). The deposit contained 79% SiO_2. KWD2 contained 3.5% Fe_2O_3, 8% Al_2O_3, 8.92% P_2O_5 and 46.7% SiO_2 (Table 3).

FTIR analyses: Bands of specific wavelengths were evident in the KWD3 deposit and showed the presence of functional groups based on vibrational frequencies: alcohols, carboxylic acid, alkynes, primary and secondary

Table 4. FTIR showing functional groups from KWD3

Frequency (cm^{-1})	Bond	Functional group
3640–3610 (s, sh)	O–H stretch, free hydroxyl	Alcohols, phenols
3500–3200 (s, b)	O–H stretch, H-bonded	Alcohols, phenols
3300–2500 (m)	O–H stretch	Carboxylic acids
3000–2850 (m)	C–H stretch	Alkanes
1500–1400 (m)	C–C stretch (in-ring)	Aromatics
1320–1000 (s)	C–O stretch	Alcohols, carboxylic acids, esters, ethers
1250–1020 (m)	C–N stretch	Aliphatic amines
1000–650 (s)	=C–H bend	Alkenes
950–910 (m)	O–H bend	Carboxylic acids
910–665 (s, b)	N–H wag	Primary, secondary amines
900–675 (s)	C–H 'oop'	Aromatics
850–550 (m)	C–Cl stretch	Alkyl halides
700–610 (b, s)	–C (triple bond) C–H: C–H bend	Alkynes
690–515 (m)	C–Br stretch	Alkyl halides

amines (Table 4). The IR spectra were compared to the database of spectra of known compounds using standard reference material[24, 25].

Scanning electron microscopy: SEM photomicrographs of the black cave wall deposit KWD3 showed the presence of (1) thin, long fibres with grainy outer surfaces of 200–600 μm length and 4–5 μm diameter (Figure 2 *a* and *b*); (2) calcified microbial filaments similar to bacterial forms with smooth outer surfaces of 2.5–5 μm diameter (Figure 2 *c*); (3) bent calcified microbial forms (Figure 2 *c*); (4) EDX of calcified filaments with Fe, O and traces of Ca and Si (Figure 2 *d*); (5) a meshwork of thin, fine and extremely long calcified filaments (Figure 2 *e*) and (6) very fine filaments (<1 μm diameter; Figure 2 *f*).

Microbiology

Microbial enumeration

Microbial cell counts on various enrichment media showed the presence of high microbial cell numbers and diverse microbial groups (Table 5). The highest number of morphologically different isolates was observed on the B4 agar followed by the NA plates. The high population densities for speleothems and wall deposits include: 4.2×10^5 on B4 agar (KWD2); 3.4×10^5 on B4 agar (KST3); 5.2×10^2 on NA (KST2) and 7.2×10^2 on SA agar (KWD1).

Identification of calcifying strains

S1–S13 were identified using standard biochemical tests in the laboratory (Table 6). They were identified as *Bacillus* sp., *Micrococci* sp. and *Staphylococcus* sp. S14 strain was identified as *Rhodococcus* sp. belonging to Actinobacteria (NCBI accession number JQ316226.1). The nucleotide-based phylogenetic tree of S14 strain *Rhodococcus* sp. suggests that it formed a major cluster with several other strains of *Rhodococcus* sp. isolated globally (Figure 3).

Experimental geomicrobiology

The optimal growth temperatures occurred at ~25°C and 14 isolates were able to precipitate calcite *in vitro* (Table 7). The minimum time for initiation of crystallization (7–14 days) differed between the isolates (Table 7). The controls consisting of flasks without inoculation of bacterial strains did not precipitate carbonate minerals. The B4 broth became turbid as bacterial growth rate increased. The pH increased with time (over a period of 35 days) from 7 to 8.8, and the bacterial growth recorded at OD_{600} also showed increased growth with time. The amount of calcite precipitated varied from 0.23 to 0.61 g. S1 strain *Bacillus* sp. precipitated the maximum amount of calcite (0.61 g) followed by S9 strain *Staphylococci* sp. (0.59 g). S14 strain *Rhodococcus* sp. precipitated 0.23 g of calcite (Table 7) (Figure 4 *a* and *b*).

SEM of the precipitated minerals by S14 strain

The *Rhodococcus* sp. S14 strain precipitated spherulites with small pores (Figure 5 *a–e*). The biominerals collected after 20 days were ~5 μm in diameter with smooth outer surfaces and pores on the spherulites were ~2.5 μm in diameter (Figure 5 *b*). In the initial stages, the crystals took the form of discs (Figure 5 *b*(i)) with a central opening that developed into cup-like structures with wide openings and layered thin calcite crusts (Figure 5*b*(ii) and *c*). As the crystal formation progressed, the opening of the cup-shaped structures began to decrease, formed spherulites (Figure 5 *d*) and later merged with other similar crystals to form coccolith-like aggregates of crystals

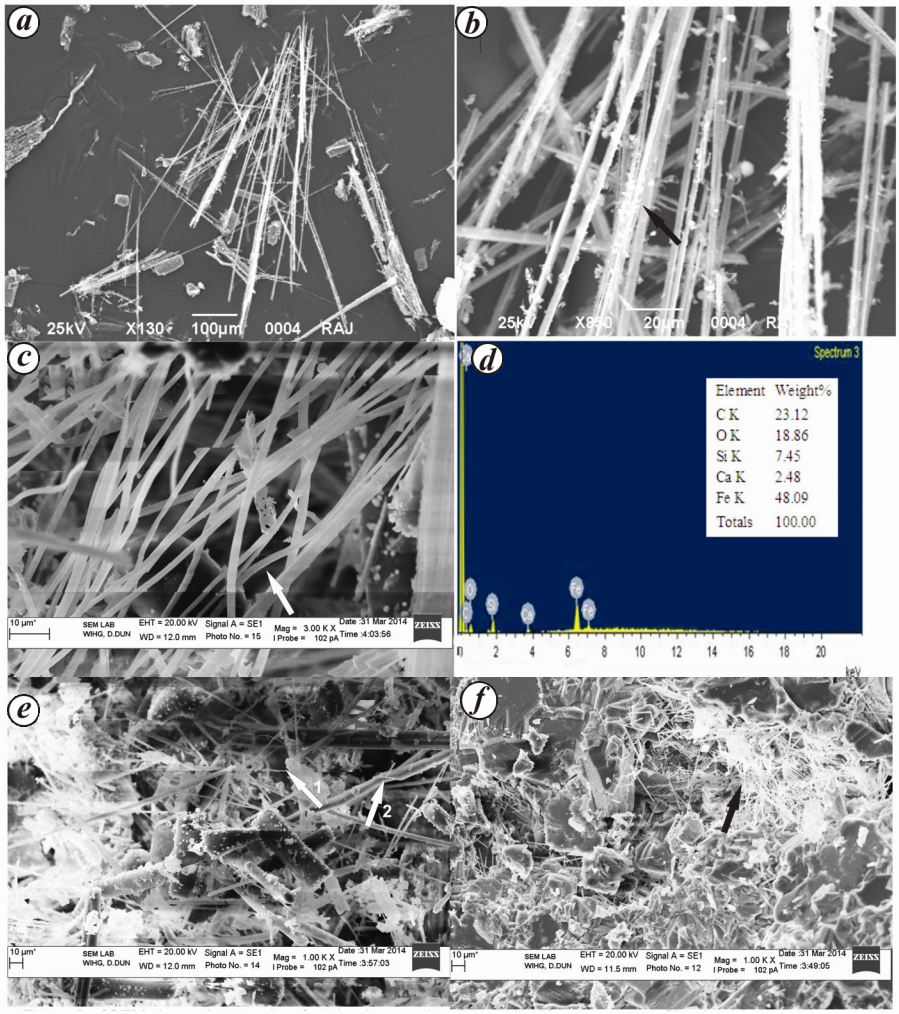

Figure 2. SEM photomicrographs of speleothem and wall deposits, Kotumsar cave. ***a***, Thin long fibres with grainy outer surfaces 200–600 µm from KWD3 wall deposit; ***b***, Enlarged structures seen in (***a***); ***c***, Calcified microbial filaments similar to bacterial forms with smooth outer surfaces 2.5–5 µm diameter in the wall deposit; bent calcified forms; ***d***, EDX of the calcified filament observed in (***c***) showing Fe, O, Ca and Si; ***e***, Meshwork of thin, fine and extremely long calcified filaments in KST1 stalactite; ***f***, Very fine filaments <1 µm diameter in KWD2 wall deposit.

(Figure 5 *e*). The biominerals collected after 35 days were ~10–25 µm in diameter with smooth outer surfaces and the pores on the spherulites were ~4 µm in diameter (Figure 5 *d*). The crystal precipitation was external to the bacterial cell wall and not intracellular. EDX of the cup-shaped structures and final precipitate showed the presence of Ca (Figure 5 *f*).

Discussion

Microorganisms are capable of carrying out mineral transformation and promote biomineralization processes[26]. The close relationships of biomineral formation with natural environments are key aspects of natural biogeochemical cycles[27–29]. Biomineralization is induced by organisms and most biominerals contain organic matrix and nano/microscale amorphous or crystalline minerals[30]. Biominerals differ from their inorganically produced counterparts in terms of shape, size, crystallinity, and isotopic and trace element geochemistry[31]. The present study shows the influence of microbes in $CaCO_3$ formation in caves. The observed evidences to support biogenicity include: (1) high microbial cell numbers, (2) presence of functional organic groups, (3) SEM documenting the presence of calcified microbial forms, and (4) *in vitro* experiments confirming the precipitation of $CaCO_3$ by *Rhodococcus* strain.

Microbes can influence mineral formation through the following ways: (a) altering the chemistry of the solution to make it supersaturated; (b) producing organic polymers that act as nucleation sites and (c) influence mineral growth by inhibiting crystal growth along certain directions, resulting in minerals with unusual shapes[32]. Cave

Table 5. Enumeration of microbes on different media

Sample no.	Isolation source	Medium	Reference	Carbon/nutrient source in the medium	Useful in the detection of microbes	Colour of the isolate	Similar isolates	Viable culturable microbes (CFU/g)
KST2	Stalactite	NA	Hi-Media	Glucose, peptone, yeast, beef extract	Heterotrophic bacteria, non-fastidious organisms	Pale white	3	5.0×10^2
KST3	Stalactite	NA	Hi-Media	"	"	Creamy-white	5	2.0×10^2
KWD1	Wall deposit	NA	Hi-Media	"	"	Light pink	4	5.2×10^2
KWD2	Wall deposit	NA	Hi-Media	"	"	Pale white	6	2.4×10^2
KWD3	Wall deposit	NA	Hi-Media	"	"	Light yellow	3	3.0×10^2
KST1	Stalactite	B4	20	Glucose, yeast, calcium acetate		Creamy-white	3	2.6×10^5
KST2	Stalactite	B4	20	"		Light yellow	5	2.0×10^5
KST3	Stalactite	B4	20	"		Pale white	3	3.4×10^5
KSM	Stalagmite	B4	20	"		Light yellow	4	2.2×10^5
KWD1	Wall deposit	B4	20	"		Creamy-white	2	1.6×10^5
KWD2	Wall deposit	B4	20	"		Reddish	7	4.2×10^5
KWD3	Wall deposit	B4	20	"		Pale white	3	1.4×10^5
KST1	Stalactite	STA	Hi-Media	Sodium thiosulphate, calcium chloride	Sulphur-metabolizing bacteria	Creamy	4	2.8×10^2
KST2	Stalactite	STA	Hi-Media	"	"	Pale white	5	0.4×10^2
KST3	Stalactite	STA	Hi-Media	"	"	Pale white	3	0.8×10^2
KSM	Stalagmite	STA	Hi-Media	"	"	Pale white	2	1.2×10^2
KWD1	Wall deposit	STA	Hi-Media	"	"	Pale white	6	3.3×10^2
KST2	Stalactite	SA	Hi-Media	Tryptone, sodium sulphite	Thermophilic sulphide-producing anaerobic microorganisms	Creamy-white	6	2.1×10^2
KST3	Stalactite	SA	Hi-Media	"	"	Yellow	7	4.0×10^2
KSM	Stalagmite	SA	Hi-Media	"	"	Yellow	9	2.0×10^2
KWD1	Wall deposit	SA	Hi-Media	"	"	Creamy-white	5	7.2×10^2
KWD2	Wall deposit	SA	Hi-Media	"	"	Light yellow	3	2.4×10^2
KWD3	Wall deposit	SA	Hi-Media	"	"	Pale white	8	3.2×10^2
KST1	Stalactite	MNA	Hi- Media	Manganous carbonate, ferrous ammonium sulphate	*Leptothrix* sp.	Creamy-white	4	1.0×10^2
KST2	Stalactite	MNA	Hi-Media	"	"	Creamy-white	5	1.6×10^2
KSM	Stalagmite	MNA	Hi-Media	"	"	Creamy-white	5	1.4×10^2
KWD1	Wall deposit	MNA	Hi-Media	"	"	Pale white	6	2.8×10^2
KWD3	Wall deposit	MNA	Hi-Media	"	"	Light yellow	4	1.2×10^2
KST1	Stalactite	Bg-11	Atla&Parks, 1993	Citric acid, ferrous ammonium citrate	*Cyanobacteria* sp.	Yellow	3	1.4×10^2
KST3	Stalactite	Bg-11	Atla&Parks, 1993	"	"	Yellow	3	2.2×10^2
KSM	Stalagmite	Bg-11	Atla&Parks, 1993	"	"	Creamy-white	2	1.6×10^2
KWD1	Wall deposit	Bg-11	Atla&Parks, 1993	"	"	Pinkish-yellow	2	4.0×10^2
KWD2	Wall deposit	Bg-11	Atla&Parks, 1993	"	"	Pale white	4	3.0×10^2
KST1	Stalactite	KIA	Hi-Media	Peptone, iron, beef, yeast, lactose, glucose	Iron bacteria, *Yersinia enterocolitica*	Creamy-white	3	3.5×10^2
KST2	Stalactite	KIA	Hi-Media	"	"	White	5	3.0×10^2
KST3	Stalactite	KIA	Hi-Media	"	"	Light red, creamy	10	3.1×10^2
KSM	Stalagmite	KIA	Hi-Media	"	"	Creamy-red	4	2.7×10^2
KWD1	Wall deposit	KIA	Hi-Media	"	"	Light pink	12	2.5×10^2
KWD2	Wall deposit	KIA	Hi-Media	"	"	Pale white	9	3.2×10^2
KWD3	Wall deposit	KIA	Hi-Media	"	"	Light pink	8	3.3×10^2
KSM	Stalagmite	IA	Hi-Media	Glucose, ammonium sulphate, calcium nitrate, thiamine dipotassium phosphate, cyanocobalamin	Gram-negative enteric bacilli	White	4	1.7×10^2
KWD3	Wall deposit	IA	Hi-Media	"	"	Pale white	5	2.0×10^2

NA, Nutrient agar; B4, B4 agar; STA, Sodium thiosulphite agar; SA, Sulphite agar; MNA, Manganese agar; Bg-11, Bg-11 agar; KIA, Kliger iron agar; IA, Iron agar.

Table 6. Identification of bacterial strains isolated from Kotumsar cave

Strain no.	Gram	Catalase	Oxidase	Urease	Anaerobiosis	$NO_3^- \rightarrow NO_2^-$	Microorganisms	Metabolism
S1	–	+	+	+	+	–	*Bacillus* sp.	Facultative anaerobes
S2	–	+	+	+	+	–	*Bacillus* sp.	Facultative anaerobes
S3	+	+	–		–	+	*Micrococci* sp.	Aerobic
S4	–	+	+	+	+	–	*Bacillus* sp.	Facultative anaerobes
S5	+	+	–	+	+	+	*Staphylococcus* sp.	Facultative anaerobes
S6	–	+	+	+	+	–	*Bacillus* sp.	Facultative anaerobes
S7	+	+	–	+	–	+	*Micrococci* sp.	Aerobic
S8	+	+	+	+	+	–	*Bacillus* sp.	Facultative anaerobes
S9	+	+	–	+	+	+	*Staphylococcus* sp.	Facultative anaerobes
S10	–	+	+	+	+	–	*Bacillus* sp.	Facultative anaerobes
S11	–	+	–		–	+	*Micrococci* sp.	Aerobic
S12	+	+	+	+	+	–	*Bacillus* sp.	Facultative anaerobes
S13	+	+	–	+	+	+	*Staphylococcus* sp.	Facultative anaerobes
S14	+	+	–	+	–	+	*Rhodococcus* sp.	Aerobic

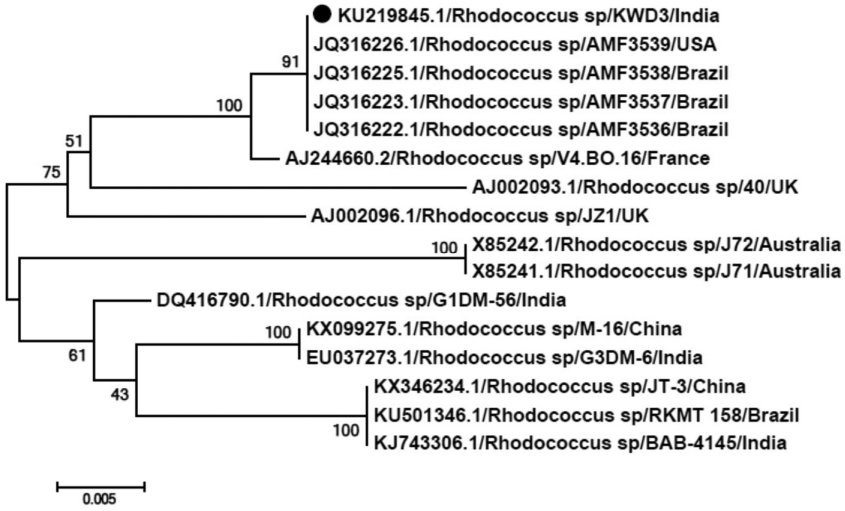

Figure 3. 16S rRNA-based tree reflecting the phylogenetic relationships of S14 strain KU219845.1 sequences and a selection of reference sequences. The phylogenetic tree was constructed using p-distance matrix of neighbor joining algorithm with 1000 bootstrap values and visualized by TreeView.

microorganisms are known to affect mineral precipitation either passively (by acting as nucleation sites) or actively (by producing enzymes or substances)[33,34].

SEM of the Kotumsar speleothems revealed fibre calcites, calcified bacterial forms and iron minerals, indicative of microbial presence. Microbial studies involving the isolation and enumeration of bacteria from the stalactites, stalagmites and cave wall deposits show high numbers and diversity of bacterial strains. The metabolic function of the identified microorganisms enhances the pH of the medium, thereby influencing calcite precipitation. In caves, such biologically induced mineralization influences the genesis of various minerals.

Biomineral formation by Rhodococcus sp. in vitro

Rhodococci sp. is an aerobic, Gram-positive, non-motile, mycolate-containing, nocardioform actinomycetes[35]. The geomicrobiological experiments performed in the laboratory showed that the isolated *Rhodococcus* strains precipitate calcite minerals *in vitro*. SEM of the precipitated material showed aggregates of bacteria. The biominerals produced by *Rhodococcus* sp. S14 strain were spherulites with small pores (Figure 5 *a* and *b*) that finally took the form of coccolith-like aggregates of crystals (Figure 5 *f*). The studied observations indicate that *Rhodococci* sp. is capable of microbe–mineral precipitation processes with different crystal morphologies during the course of their evolution. The subtle micro-environmental changes, i.e. pH increase in culture medium as a result of bacterial metabolism, observed during the experiment period may be due to the intake of carbon sources[36]. *Rhodococcus* sp. is reported to utilize acetate that can increase the pH of the medium, which helps in carbonate precipitation[36]. Although members of *Rhodococcus* genera are known to produce calcite[37,38], the morphology of the crystals induced by S14 strain in the present study is unique and has

Table 7. *In vitro* calcite precipitation by bacterial strains isolated from Kotumsar cave

Sample	Strain	Gram reaction	Isolate type	pH (days)					OD_{660} (days)					Calcite (g)
				7	14	21	28	35	7	14	21	28	35	
KST1	S1	–	*Bacilli*	7	7.24	6.93	7.8	8.4	2.063	2.01	2.03	2.061	2.126	0.61
KST1	S2	–	*Bacilli*	7.2	7.43	7.86	7.89	7.98	1.862	1.962	2.06	2.088	2.134	0.56
KST2	S3	+	*Cocci*	7.2	6.8	7.82	7.79	6.8	1.442	1.732	1.968	2.06	2.129	0.45
KST2	S4	–	*Bacilli*	7.1	7.36	7.9	8.63	8.45	2.028	1.997	2	2.085	2.13	0.57
KST3	S5	+	*Staphylococci*	7	7.21	7.8	8	8.1	1.262	1.932	1.986	1.924	2.003	0.44
KST3	S6	–	*Bacilli*	6.93	7.16	7.69	8.44	8.85	0.608	2.106	1.892	1.906	2.13	0.45
KSM	S7	+	*Cocci*	7.1	7.2	7.3	7.5	8.1	0.882	0.439	0.413	0.753	0.688	0.06
KSM	S8	+	*Bacilli*	7.1	7.5	7.7	8.15	8.18	0.474	1.564	1.167	2.066	2.197	0.55
KWD1	S9	+	*Staphylococci*	7	7.22	7.5	8.16	8.9	1.678	1.459	1.539	2.13	2.203	0.59
KWD1	S10	–	*Bacilli*	7.4	7.68	8.07	8.27	8.2	1.821	1.948	2.135	2.061	2.112	0.44
KWD2	S11	–	*Cocci*	7.44	7.6	7.94	7.5	7.59	2.107	2	2.021	1.972	2.006	0.57
KWD2	S12	+	*Bacilli*	6.9	7.6	7.93	7.84	8	1.694	2.059	1.895	2.026	2.091	0.39
KWD3	S13	+	*Staphylococci*	6.69	7.7	7.6	8.16	7.3	1.458	2.196	2.116	2.128	2.209	0.35
KWD3	S14	+	*Rhodococcus*	7.48	7.35	7.81	7.84	8.1	0.303	2.206	1.968	2.158	2.206	0.23

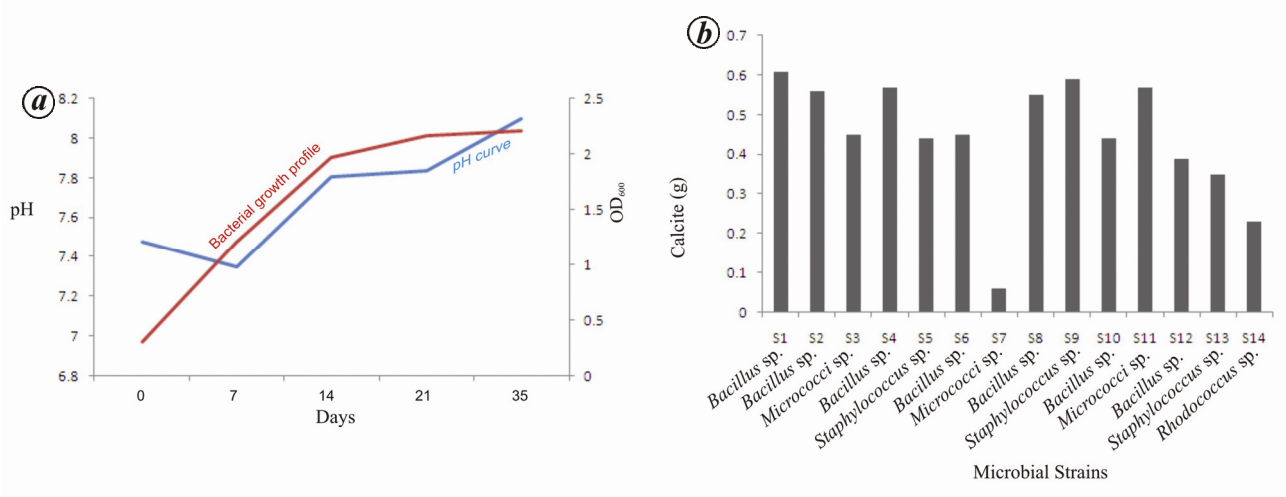

Figure 4. Graphs showing results of experimental geomicrobiology. ***a***, pH profile of *Rhodococci* sp. S14 strain showing increase in pH with the number of days of incubation and increase in bacterial growth with the number of days of incubation measured spectrophotometrically at OD_{600}. ***b***, Amount of calcite precipitated by the strains S1 to S14 *in vitro* at the end of 35 days of incubation.

not been reported so far to the best of our knowledge. The biominerals were precipitated on the *Rhodococci* sp. cell walls, which possibly acted as nucleation sites[39–41]. The external cell surfaces of *Rhodococci* sp. and their composition is important for the biomineralization process which influences the mineralogy and morphology of calcite crystals precipitated[42]. The observed biominerals were spherulites, discs and cup-shaped structures that appeared either in isolation or clusters. Majority of the crystals formed *in vitro* had outer grainy surface. It is inferred that the spherulites/coccolith formation may be the result of progressive calcification processes. Similar studies reported on *Rhodococci* sp. isolated from Grotta dei Cervi, Italy produced vaterite and calcite[37].

Another *in vitro* study reported the formation of desert-roses by *Rhodococci* sp.[43]. In caves, long-term, microbial-driven metabolic processes may be important for carbonate precipitation. EPS production, microbial cell aggregates and calcium concentration are important in bio-precipitation processes[44]. Studies have reported that *R. globerulus* and *R. erythropolis* strains produce mycolic acids which influence cell-wall properties, with hydrophobic cell surfaces that produce differences in carbonate mineral morphologies[36].

Rhodococci sp. metabolism and calcite precipitation

In heterotrophic bacteria, some processes involved in their intermediary metabolism are responsible for bioprecipitation[45–48]. There are two ways a microbe can precipitate $CaCO_3$ – through the heterotrophic pathway and the other is an autotrophic pathway[49]. It could be proposed that the *Rhodococci* sp. follows the ammonification,

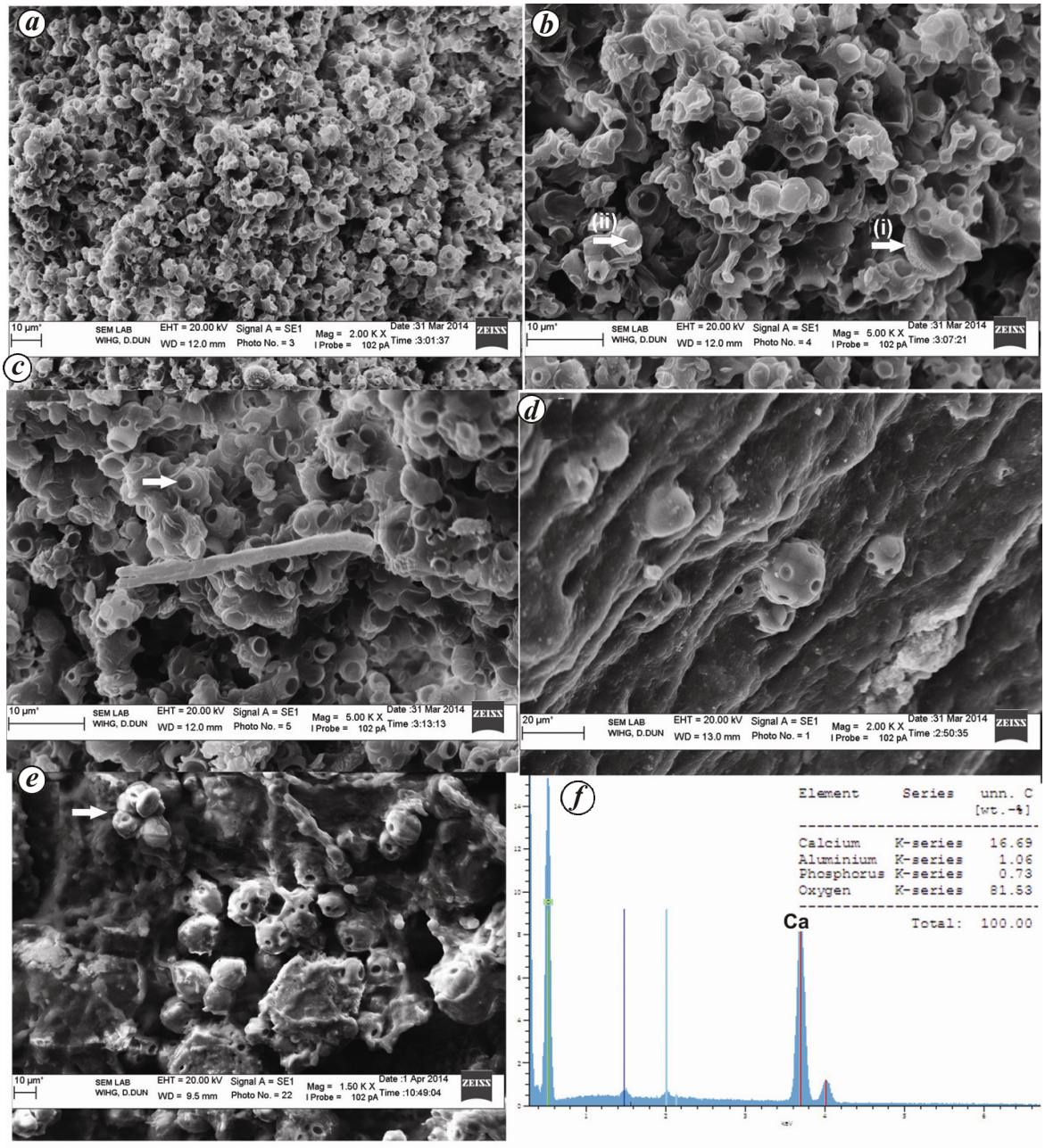

Figure 5. SEM photomicrographs of calcite precipitated by *Rhodococci* sp. strain S14 in B4 medium. ***a***, Precipitates after 20 days of incubation; ***b***, Precipitate 5 µm in diameter, note the inner smooth surfaces, crystals take the form of discs with a central opening developing into cup-like structures with wide openings (i) and thin crusts (ii); ***c***, Thin crusts of cup-like calcite structures; ***d***, Spherulites noticed after 35 days; ***e***, Similar spherulites merge to form coccolith-like aggregates of crystals with pores; pores on the spherulites are ~4 µm in diameter; ***f***, EDX of the precipitate in (***e***) showing Ca peak.

nitrate reduction and urea degradation pathway[50]. Actinobacteria are significant in cave biomineralization processes. The biomineral formation abilities of actinobacteria can help understand their role in cave biogeochemical cycles.

Conclusion

This study showed that *Rhodococci* sp. is capable of forming calcite through its metabolic activities. The observations imply that microbial metabolism influences the formation of secondary mineral deposits in cave ecosystems. The commercial potential of *Rhodococci* sp. is due to its ability to transform and degrade a range of chemicals. It has potential applications in environmental as well as industrial biotechnology. It is also capable of synthesizing surfactants, flocculants, amides and polymers.

1. Ikner, L. A., Toomey, R. S., Nolan, G., Neilson, J. W., Pryor, B. M. and Maier, R., Culturable microbial diversity and the impact of

tourism in Kartchner Caverns, Arizona. *Microb. Ecol*., 2007, **53**, 30–42.
2. Shapiro, J. and Pringle, A., Anthropogenic influences on the diversity of fungi isolated from caves in Kentucky and Tennessee. *Am. Midl. Nat.*, 2010, **163**, 76–86.
3. Adetutu, E. M., Thorpe, K., Bourne, S., Cao, X., Shahsavari, E., Kirby, G. and Ball, A. S., Phylogenetic diversity of fungal communities in areas accessible and not accessible to tourists in Naracoorte Caves. *Mycologia*, 2011, **103**, 959–968.
4. Barton, H. A. and Jurado, V., What's up down there? Microbial diversity in caves. *Microbe*, 2007, **2**, 132–138.
5. Chafetz, H. S., Bacterially induced precipitates of calcium carbonate and lithification of microbial mats. In *Biostabilization of Sediments* (eds Krumbein, W. E., Paterson, D. M. and Stal, L. J.), Universitat Oldenburg, Germany, 1994, pp. 149–163.
6. Ehrlich, H. L., *Geomicrobiology*, Marcel Dekker, Inc, New York, 1996, p. 719.
7. Rivadeneyra, M. A., Delgado, G., Ramos-Cormenzana, A. and Delgado, R., Biomineralisation of carbonates by *Halomonas eurihalina* in solid and liquid media with different salinities: crystal formation sequence. *Res. Microbiol.*, 1998, **149**, 277–287.
8. Cacchio, P., Ercole, C., Contento, R., Cappuccio, G., Martinez, M. P., Del Gallo, M. and Lepidi, A., Involvement of bacteria in the origin of a newly described speleothem in the gypsum cave of Grave Grubbo (Crotone, Italy). *J. Cave Karst. Stud.*, 2012, **74**(1), 7–18.
9. Miller, A. Z., Dionísio, A., Jurado, V., Cuezva, S., Sanchez-Moral, S., Cañaveras, J. C. and Saiz-Jimenez, C., Biomineralization by cave dwelling microorganisms. In *Advances in Geochemistry Research* (ed. Sanjurjo Sanchéz, J.), Nova Science Publishers, New York, 2013, pp. 77–105.
10. Baskar, S., Routh, J., Baskar, R., Kumar, A., Miettinen, H. and Itaevaara, M., Evidences for microbial precipitation of calcite in speleothems from Krem Syndai in Jaintia Hills, Meghalaya, India. *Geomicrobiol. J.*, 2016, **33**(10), 906–933.
11. Lichtinger, T., Reiss, G. and Benz, R., Biochemical identification and biophysical characterization of a channel-forming protein from *Rhodococcus erythropolis*. *J. Bacteriol*., 2000, **182**(3), 764–770.
12. McLeod, M. *et al*., The complete genome of *Rhodococcus* sp. RHA1 provides insights into a catabolic powerhouse. *Proc. Natl. Acad. Sci. USA*, 2006, **103**, 15582–15587.
13. Amann, R. I., Ludwig, W. and Schleifer, K. H., Phylogenetic identification and *in situ* detection of individual microbial cells without cultivation. *Microbiol. Rev.*, 1995, **59**, 143–169.
14. Donachie, S. P., Foster, J. S. and Brown, M. V., Culture clash: challenging the dogma of microbial diversity. *ISME J.*, 2007, **1**, 97–102.
15. De Leo, F., Iero, A., Zammit, G. and Urzì, C., Chemoorganotrophic bacteria isolated from biodeteriorated surfaces in cave and catacombs. *Int. J. Speleol.*, 2012, **41**(2), 125–136.
16. Sankhyan, A. R., Dewangan, L. N., Sahoo, R. H., Chakravarty, R. and Chatterjee, R., Early prehistoric signatures of man in Bastar region, Central India. *Curr. Sci*., 2011, **101**(9), 1146–1149.
17. Diwan, H. D., Gupta, M. P. and Bandhu, J., Perspective geomorphic analysis of Kotumsar karstic cave zone, Kanger Valley, Chhattisgarh (India). In XVII International Symposium on Biospeleology, Raipur, Abstr., 2004, p. 41.
18. Biswas, J., Kotumsar cave biodiversity: a review of cavernicoles and their troglobiotic traits. *Biodivers. Conserv*., 2010, **19**(1), 275–289.
19. Yadava, M. G., Sarswat, K. S. and Ramesh, R., Evidences of early human occupation in the limestone caves of Bastar, Chhattisgarh. *Curr. Sci.*, 2007, **92**(6), 25.
20. Boquet, E., Boronat, A. and Ramos-Cormenza, A., Production of calcite (calcium carbonate) crystals by soil bacteria is a general phenomenon. *Nature*, 1973, **246**, 527–529.
21. Altschul, S. F., Madden, T. L., Schaffer, A. J., Zhang, J., Zhang, Z., Miller, W. and Lipman, D. J., Gapped BLAST and PSI-BLAST: A new generation of protein database search programs. *Nucleic Acids Res*., 1997, **25**, 3389–3402.
22. Tamura, K., Peterson, D., Peterson, N., Stecher, G., Nei, M. and Kumar, S., MEGA5: Molecular evolutionary genetics analysis using maximum likelihood, evolutionary distance, and maximum parsimony methods. *Mol. Biol. Evol.*, 2011, **28**, 2731–2739.
23. Hall, T. A., BioEdit: a user-friendly biological sequence alignment editor and analysis program for Windows 95/98/NT. *Nucleic Acids Symp. Ser*., 1999, **41**, 95–98.
24. Sharma, Y. R., *Elementary Organic Spectroscopy: Principles and Chemical Applications*, S. Chand Publ, New Delhi, 1989, p. 294.
25. Robinson, J. W., Frame, E. M. S. and Frame II, G. M., In *Undergraduate Instrumental Analysis*, CRC Press, Taylor and Francis Group, Boca Raton, 2004, 6th edn, p. 1079.
26. Hofmann, B. A., Farmer, J. D., von Blanckenburg, F. and Fallick, A. E., Subsurface filamentous fabrics: an evolution of origins based on morphological and geochemical criteria, with implications for exopaleontology. *Astrobiology*, 2008, **8**, 87–117.
27. Nealson, K. H. and Stahl, D. A., Microorganisms and biogeochemical cycles; what can we learn from layered microbial communities? In *Geomicrobiology: Interactions between Microbes and Minerals* (eds Banfield, J. F. and Nealson, K. H.), Mineralogical Society of America, Washington, DC, 1997, vol. 35, pp. 5–34.
28. Newman, D. K. and Banfield, J. F., Geomicrobiology: how molecular-scale interactions underpin geochemical systems. *Science*, 2002, **296**, 1071–1077.
29. Van Cappellen, Biomineralization and global biogeochemical cycles. In *Biomineralization, Rev. Mineralogy and Geochemistry* (eds Dove, P. M., De Yoreo, J. J. and Weiner, S.), 2003, vol. 54, pp. 357–381.
30. Bauerlein, E., Biomineralization of unicellular organisms: an unusual membrane biochemistry for the production of inorganic nano- and microstructures. *Angew. Chem., Int. Ed. Engl.*, 2003, **42**(6), 614–641.
31. Weiner, S. and Dove, P. M., An overview of biomineralization processes and the problem of the vital effect. *Rev. Mineral. Geochem*., 2003, **54**, 1–29.
32. Benzerara, K., Miot, J., Morin, G., Ona-Nguema, G., Skouri-Panet, F. and Ferard, C., Significance, mechanisms and environmental implications of microbial biomineralization. *C. R. Geosci*., 2011, **343**, 160–167.
33. Northup, D. E. and Lavoie, K. H., Geomicrobiology of caves: a review. *Geomicrobiol. J.*, 2001, **18**, 199–222.
34. Jones, B., Speleothems in a wave-cut notch, Cayman Brac, British West Indies: the integrated product of subaerial precipitation, dissolution, and microbes. *Sediment. Geol.*, 2010, **232**, 15–34.
35. Goodfellow, M., The actinomycetes I. Suprageneric classification of actinomycetes. In *Bergey's Manual of Systematic Bacteriology* (eds Williams, S. T., Sharpe, M. E. and Holt, J. G.), Williams & Wilkins, Baltimore, 1989, vol. 4, pp. 2333–2339.
36. Rusznyák, A. *et al.*, Calcite biomineralization by bacterial isolates from the recently discovered pristine karstic Herrenberg Cave. *Appl. Environ. Microbiol.*, 2012, **78**, 115–1167.
37. Groth, I., Schumann, P., Laiz, L., Sanchez-Moral, S., Cañaveras, J. C. and Saiz-Jimenez, C., Geomicrobiological study of the Grotta dei Cervi, Porto Badisco, Italy. *Geomicrobiol. J*., 2001, **18**, 241–258.
38. Cacchio, P., Ercole, C., Cappuccio, G. and Lepidi, A., $CaCO_3$ precipitation by bacterial strains isolated from a limestone cave and from a loamy soil. *Geomicrobiol. J.*, 2003, **20**, 85–98.
39. Van Lith, Y., Warthmann, R., Vasconcelos, C. and McKenzie, J., Microbial fossilization in carbonate sediments: a result of the bacterial surface involvement in dolomite precipitation. *Sedimentology*, 2003, **50**, 237–245.

40. Dupraz, C., Vissher, P. T., Baumgartner, L. K. and Reid, R. P., Microbe–mineral interactions: early carbonate precipitation in a hypersaline lake (Eleuthera Island, Bahamas). *Sedimentology*, 2004, **51**, 745–765.
41. Aloisi, G., Gloter, A., Krüger, M., Wallmann, K., Guyot, F. and Zuddas, P., Nucleation of calcium carbonate on bacterial nanoglobules. *Geology*, 2006, **34**, 1017–1020.
42. Braissant, O., Cailleau, G., Dupraz, C. and Verrecchia, A. P., Bacterially induced mineralization of calcium carbonate in terrestrial environments: the role of exopolysaccharides and amino acids. *J. Sediment. Res.*, 2003, **73**, 485–490.
43. Gonzalez-Muñoz, M. T., Chekroun, K. B., Aboud, A. B., Arias, J. M. and Rodriguez-Gallego, M., Bacterially induced Mg-calcite formation: role of Mg^{2+} in development of crystal morphology. *J. Sediment. Res*., 2000, **70**, 559–564.
44. Portillo, M. C., Porca, E., Cuezva, S., Canaveras, J. C., Sanchez-Moral, S. and Gonzalez, J. M., Is the availability of different nutrients a critical factor for the impact of bacteria on subterraneous carbon budgets? *Naturwissenschaften*, 2009, **96**, 1035–1042.
45. Beveridge, T. J., Role of cellular design in bacterial metal accumulation and mineralization. *Annu. Rev. Microbiol.*, 1989, **43**, 147–171.
46. Castanier, S., Metayer-Levrel, G. L., Orial, G., Loubiere, J. F. and Perthuisot, J. P., Bacterial carbonatogenesis and applications to preservation and restoration of historic property. In *Microbes and Art: The Role of Microbial Communities in the Degradation and Protection of Cultural Heritage* (eds Ciferri, O., Tiano, P. and Mastromei, G.), Plenum, New York, 2000, pp. 201–216.
47. Wright, D. T. and Oren, A., Nonphotosynthetic bacteria and the formation of carbonates and evaporites through time. *Geomicrobiol. J*., 2005, **22**, 27–53.
48. Gadd, M., Metals, minerals and microbes: geomicrobiology and bioremediation. *Microbiology*, 2010, **156**(3), 609–643.
49. Castanier, S., Le M´etayer-Levrel, G. and Perthuisot, J. P., Ca-carbonates precipitation and limestone genesis – the microbiogeologist point of view. *Sediment. Geol.*, 1999, **126**, 9–23.
50. Fujita, Y., Ferris, F. G., Lawson, R. D., Colwell, F. S. and Smith, R. W., Calcium carbonate precipitation by ureolytic subsurface bacteria. *Geomicrobiol. J*., 2000, **17**, 305–318.

ACKNOWLEDGEMENTS. We thank Prof. Minakshi Prasad, Department of Animal Biotechnology, College of Veterinary Sciences, LLR University of Animal and Veterinary Sciences, GJUST, Hisar; Panjab Agricultural University, Patiala; Wadia Institute of Himalayan Geology, Dehradun and geneOmbio Technologies, Pune for analyses and research facilities. Dr Jayant Biswas and Devender Mudgil helped in the field work. S.C. thanks UGC-BSR for fellowship.

Received 14 February 2017; accepted 14 September 2017

doi: 10.18520/cs/v114/i05/1063-1074